1-1997

Variations in the Frequency-Magnitude Distribution with Depth in Two Volcanic Areas: Mount St. Helens, Washington, and Mt. Spurr, Alaska

Stefan Wiemer
Universtiy of Alaska Fairbanks

Stephen R. McNutt
Universtiy of Alaska Fairbanks, smcnutt@usf.edu

GEOPHYSICAL RESEARCH LETTERS, VOL. 24, NO. 2, PAGES 189-192, JANUARY 15, 1997

Variations in the frequency-magnitude distribution with depth in two volcanic areas: Mount St. Helens, Washington, and Mt. Spurr, Alaska

Stefan Wiemer and Stephen R. McNutt[1]

Geophysical Institute, University of Alaska Fairbanks, Fairbanks, Alaska

Abstract. The frequency-magnitude distribution of earthquakes, characterized using the *b*-value, is examined as a function of space beneath Mount St. Helens (1988-1996), and Mt. Spurr (1991-1995). At Mount St. Helens, two volumes of anomalously high *b* (b >1.3) can be observed at depths of 2.6-3.6 km below the crater floor and below 6.4 km. These anomalies coincide with (1) the depth of vesiculation of ascending magma, and (2) the suggested location of a magma chamber at Mount St. Helens. Study of Mt. Spurr reveals an area of high *b*-value (*b* ≥1.3) at a depth of about 2.3-4.5 km below the crater floor of the active vent Crater Peak. We propose that the higher material heterogeneity in the vicinity of a magma chamber or conduit due to vesiculation of the ascending magma is the main cause of the increased *b*-value at shallow depths. Alternatively, interaction of magma with groundwater may have increased pore pressure and lowered the effective stress. The deeper anomaly at Mount St. Helens is likely caused by high thermal stress gradients in the vicinity of the magma chamber. Our results indicate that detailed mapping of the frequency-magnitude distribution can be used as a tool to trace vesiculation and locate active magma chambers.

Introduction

Many studies of the frequency-magnitude distribution (FMD) as a function of time, space, and depth have been conducted since *Ishimoto and Iida* [1939] and *Gutenberg and Richter* [1944] introduced the relation between the frequency of occurrence and magnitude of earthquakes: $log_{10}N=a-bM$, where *N* is the cumulative number of earthquakes having magnitudes larger than M, and *a* and *b* are constants. The slope, or *b*-value, has been shown in laboratory studies, mines, and numerical simulations to depend on environmental conditions. Several authors explained variations in the FMD as being caused primarily by material properties [e.g. heterogeneity, *Mogi*, 1962], magnitude of applied shear stress or effective stress [*Urbancic* et al., 1992], and temperature gradient [*Warren and Latham*, 1970].

Volcanic areas are commonly reported to have high *b*-values [e.g. *Warren and Latham*, 1970], and some authors have investigated *b*-value changes in volcanic areas as a function of time [e.g. *Zobin*, 1979]. In the vicinity of magma chambers all three of the aforementioned mechanisms favor a high *b*-value. In general, volcanoes have high heterogeneity because of layering of lava flows and ash, the presence of cooling cracks, dikes and sills, and high thermal gradients in the vicinity of magma. Of course, in magma itself no earthquakes should be produced due to the limited shear strength of molten material. Magma chambers at stratovolcanoes are generally equant in shape, and on the order of 1-20 km^3 in size [*Iyer*, 1984]. Their depths are mapped at about 5-20 km based on tomography, S-wave screening, and post-eruption seismicity [*Iyer*, 1984]. We chose Mount St. Helens as our first target for a detailed mapping of the FMD because its eruptions are some of the best documented, it has a high quality earthquake catalog, and the internal structure of the magmatic system has been studied by a number of researchers. We then applied our method to a similar stratovolcano, Mt. Spurr, where the volcanic plumbing system is largely unknown.

[1]Also at Alaska Volcano Observatory

Paper number 96GL03779.
0094-8534/97/96GL-03779$05.00

Data and Method

Mount St. Helens: Volcano-tectonic (VT; also known as high frequency or A-type) events were selected from the earthquake catalog of the University of Washington. Earthquakes were not relocated or reprocessed beyond their catalog entries. Following the results of *Moran* [1994] we decided to use data spanning the period 1988 through January 1996. During this time no major eruptions occurred at Mount St. Helens. The magnitude range is 0.4 to 2.8 and the 1674 events range in depth from 0 to 10 km. The overall *b*-value from 1988 onward is 0.96±0.06, a value close to the average world-wide *b*-value observed in the seismogenic crust. Using FMD plots we estimate the magnitude of completeness threshold as M_{comp}=0.4. On average, the RMS residual is 0.1±0.08 s, 10 stations reported, 13 phases were picked, and the average error in the hypocenter for our data set is 0.65 km. We chose zero depth for Mount St. Helens data as the crater floor of the volcano (1.9 km above sea level).

Mt. Spurr: Mt. Spurr, an andesitic stratovolcano located in Cook Inlet, Alaska, erupted three times in the summer of 1992 through the active vent Crater Peak [*Alaska Volcano Observatory*, 1993]. Seismicity beneath the active vent Crater Peak dips to the SSW, suggesting that the magmatic conduit dips to the SSW [*Power et al.*, 1995]. Long-period earthquakes occurred at depths of 20-40 km, suggesting fluid pressurization; volcanic tremor occurred in the upper 1 km, presumably in the shallow conduit, and a post-eruption earthquake swarm at 5-10 km depths may indicate the top part of the magma chamber [*Power et al.*, 1995]. We use the data set of VT earthquakes recorded by the Alaska Volcano Observatory (AVO) with M_{comp}=0.1. The period 1991-1995 includes all three 1992 eruptions of Mt. Spurr. Overall, these data contain 643 events within about 2 km of Crater Peak and spanning a magnitude range from 0.1 to 2.2. On average, 12 phases were reported with an RMS residual of 0.12±0.07 s. Events analyzed ranged from 0 to 12 km in depth. For the Spurr data set, zero depth refers to the floor of Crater Peak at 1.98 km above sea level. Note that the reference datum is nearly the same for the two volcanoes, which facilitates comparison.

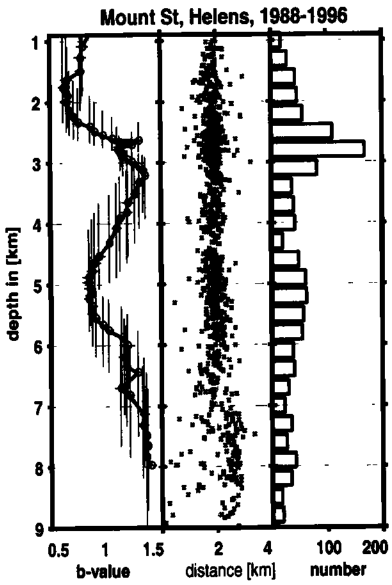

Figure 1. Left panel: b-value as a function of depth for Mount St. Helens. Horizontal bars indicate the uncertainty in b, vertical bars represent the depth range sampled. Center panel: Cross-section view, north-south trending, of the seismicity at Mount St. Helens from 1988-1996. The cross-section is 0.5 km wide and cuts through the center of Mount St. Helens. Right panel: Histogram of the depth of the seismicity at Mount St. Helens. Each bin is 0.5 km in depth.

We estimate the b-value by both the maximum likelihood and the weighted least squares methods, because different methods have different advantages and by comparing two methods we can ensure that our results are independent of the method used [*Bender*, 1983]. The b-value is estimated in sliding depth windows containing 100 or 200 earthquakes which are then displayed in vertical cross-sections. To visualize the b-value distribution as a function of space in more detail, we project all earthquakes using several one-kilometer wide vertical cross-sections. We create a dense grid with a grid spacing of 0.1 km and sample the 150 nearest earthquakes to each grid point. The volumes sampled thus represent overlapping, horizontal cylindrical volumes of varying radius, each containing 100 earthquakes. The b-value is then estimated for each volume and we assign each b-value a color. Red colors indicate high b-values, blue low b-values. For details on the techniques to estimate b see *Wiemer and Benoit* [1996].

Results

Mount St. Helens: The b-values as a function of depth, using the sliding window analysis for the Mount St. Helens catalog, are presented in Figure 1. The center panel shows a north-south cross-section view of the seismicity. The cross-section is 3 km long, 1 km wide and cuts through the center of the dome. Each of the FMD's used to calculate b contained 200 earthquakes. The b-value as a function of depth (left panel, Figure 1) is low ($b \leq 0.8$) from 0.7-2.6 km and from 3.6-6.4 km, and high ($b \geq 1.2$) from 2.6-3.6 km and from 6.4-8.0 km. Below this depth the density of earthquakes is too low to permit analysis. The right panel of Figure 1 shows a histogram of the depth distribution of the events, each bin extending 0.5 km in depth. The anomalous region of b=1.2 at 2.6-3.6 km depth correlates with an increased number of earthquakes at this depth. At greater depth no noticeable increase in the number of events is visible, despite the increased b-value. We verified our results by comparing FMD's at different depths. The b-value for earthquakes at a depths of 1-2.3 km is 0.6±0.05, and at the depth range 2.8-3.6 km is b=1.36±0.04. Both curves contain about 200 earthquakes and follow closely the linear Gutenberg-Richter distribution. The two distributions are significantly different at the 99% confidence limit using the test of *Utsu* [1992]. We are therefore confident that the distribution of b-values with depth as shown in Figure 1 is real and is not caused by computational artifacts.

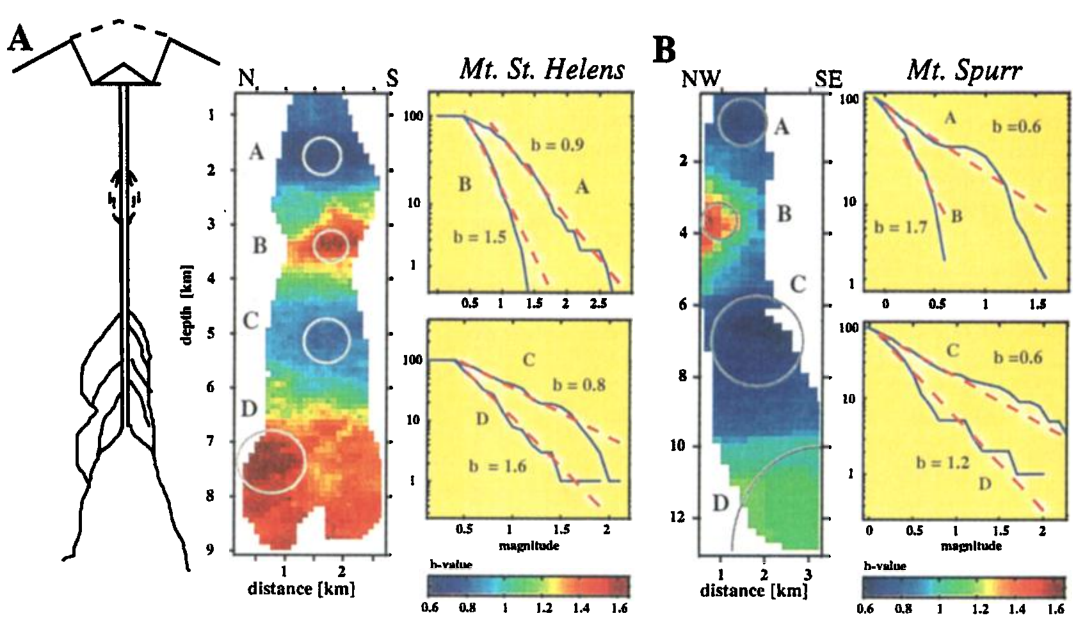

Figure 2. A) Image showing the distribution of b-values in a vertical N-S trending cross-section through Mount St. Helens. The black line drawing represents a schematic view of the Mount St. Helens systems by Pallister et al. [1992]. For four volumes (labeled A-D), the FMD is plotted on the right. B) Image showing the distribution of b-values in a vertical NW-SE trending cross-section through Crater Peak.

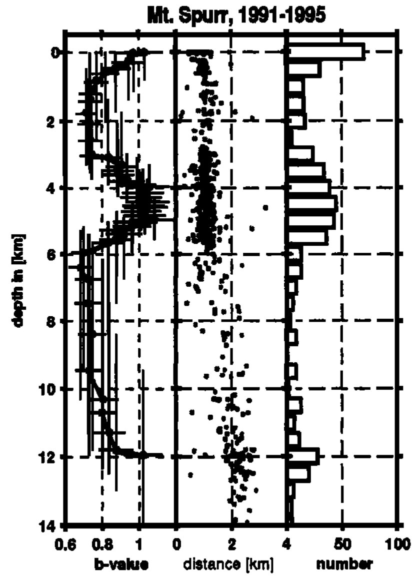

Figure 3. Same as Figure 1 for Mt. Spurr.

Using a 0.1 km grid, we map out the spatial distributions in a two dimensional view (Fig. 2A). The most outstanding anomalies are a volume of high *b*-values (red colors) at a depth of 2.7-3.8 km and a volume of high *b*-values at a depth of about 6.7-9.0 km. For both regions of increased *b* the anomalies are significantly different from the remainder of the data at the 99% confidence limit. The result of the cross-section analysis (Fig. 2A) confirms the *b*-value as a function of depth curve (Fig.1). The FMD is shown for four cylindrical volumes in the right panel of Figure 2A. The volumes (labeled A-D in Fig. 2A) were chosen to represent regions of extremely low and high *b*-value. It is clear that the distributions are distinctly different. Regions with a high *b* do not contain any events with M>1.5, whereas the low *b*-value regions contain events up to M=2.8.

Mt. Spurr: At Mt. Spurr the analysis of the FMD as a function of depth using the moving window technique for the Crater Peak seismicity (Fig. 3, left panel) shows a low *b*-value at the surface, which remains at a minimum of *b*=0.75 to about 2 km depth. A sharp peak between depths of 2.9-3.9 km (*b*=1.2) can be observed, after which *b* then drops again. The number of events in each depth bin (Fig. 3) resembles closely the distribution of *b* with depth. The spatial distribution of the FMD at Crater Peak was investigated using a SW-NE trending cross-section with a length of 3 km and a width of 2 km (Fig. 3, center panel). One outstanding region of anomalously high *b*-values can be observed at a depth of about 2.3-4.5 km depth underneath Crater Peak (Fig. 2B). The *b*-value in this region (*b*=1.8) is almost twice the normal *b*. The increase in *b* at this depth is significant at the 99% confidence limit. We show four FMD's that represent the extreme values (A-D in Figure 2B). The anomalous region at 3.2 km depth (B) cannot sustain earthquakes larger than M=0.6, whereas at other depths events with M_{max}=2.2 occur. An increase of *b* at 10.8 km depth can be observed in both the cross-section (Fig. 2B) and the *b*-value versus depth curve (Fig. 3). Unlike Mount St. Helens, Mt. Spurr has deeper seismicity extending to depths of >40 km. We obtained a *b*-value of 1.67 for the 80 events between 20 and 40 km depth. Petrologic evidence [*Nye et al.*, 1995] suggests the existence of a deep (>20 km) magma chamber at Spurr, in agreement with the high *b*-value.

Discussion and Conclusions

Our results show that the *b*-value varies significantly as a function of depth (Figs. 1 and 3) and location (Figs. 2A and 2B) under the two volcanoes investigated. The detailed analysis of the FMD is capable of resolving two distinctly different areas: (1) volumes containing average to low *b*-values (*b*=0.8±0.2), and (2) volumes containing high *b*-value anomalies (*b*=1.5±0.3). Regions of high *b*-value in our analysis are characterized by an increased number of events (Figs. 1 and 3), and typically have a largest event one magnitude unit smaller than the surrounding regions. Based on these observations we believe it is incorrect to assume that volcanic areas can simply be characterized by an overall higher *b*-value. Instead we propose that anomalously high *b*-value pockets exist in a crust otherwise described by a average or normal *b*-value. Our results emphasize the heterogeneous properties of the crust that can be studied given high quality earthquake catalogs.

For Mount St. Helens we find that the two volumes with anomalously high *b*-value coincide in location with a suggested shallow magma reservoir or zone of vesiculation and a deeper magma reservoir. The shallow anomaly at depths of 2.6-3.6 km below the dome of Mount St. Helens coincides with a zone believed altered by vesiculation and disruption of the ascending magma [*Pallister et al.*, 1992; *Chadwick et al.* 1988]. The high *b*-value anomaly at >7 km below the dome of Mount St. Helens coincides with the proposed main magma reservoir as derived from the earthquake-free zone that is surrounded by hypocenters, the orientation of the stress field at this depth [*Moran*, 1994; *Scandone and Malone*, 1985; *Barker and Malone*, 1991], and tomographic results [*Lees*, 1992]. *Lees* [1992] observed a 7 percent change in velocity at depths of 7-10 km. Using data from the period 1988-1993, *Moran* [1994] showed changes in the orientation of the stress field of up to 80° that may indicate the re-pressurization of a magma chamber at these depths.

The plumbing system of Mt. Spurr is poorly understood. The cross-section and depth slice analyses of the FMD (Figs. 2B and 3) show an increased *b*-value at a depth of 2.3-4.5 km underneath Crater Peak. Based on the similarity between the Mount St. Helens and Mt. Spurr analyses (Figs. 2A and 2B), we speculate that vesiculation permanently altered the rock surrounding the conduit at a depth of about 3-4 km underneath the active vent Crater Peak. The increase in *b* at depths below 10.8 km (Figs. 2B and 3) could be caused by a deeper magma reservoir.

The cause for the anomalously high *b*-values regions under both volcanoes cannot be resolved with certainty at this point. It is possible that all three proposed mechanisms (temperature, stress, and heterogeneity) are jointly responsible for the increase in the *b*-value. The depth of the observed shallow anomalies at both volcanoes coincides approximately with petrological evidence for the vesiculation of ascending magma containing 4 wt.% H_2O at about 4 km [*Eichelberger*, 1995]. We speculate that this marks the depth at which the vesiculation of the ascending magma causes the surrounding rock to fracture, thus increasing the crack density or heterogeneity of the material and consequently shifting the fractal distribution of events towards higher *b*-values [*Main*, 1987]. Alternatively, interaction of magma with groundwater may increase pore pressure at this depth and lower the effective stress. Open cracks are known to exist at depths of 3 km or so, and these would facilitate groundwater movement. If our interpretation is correct, the permanent trace left behind by vesiculation and thermal cracking should be detectable by our method at many andesitic volcanoes.

To explain the increase in *b* observed in the vicinity of the main magma chamber at greater depth, we suggest that an increase in the material heterogeneity in the rock surrounding the magma chamber is caused by thermal cracking and high stresses. This interpretation is consistent with the observed decrease in P and S-wave velocity at this depth [*Lees,* 1992]. The maximum magnitude of events observed in the high *b*-value zones translates into a maximum rupture length of about 70 m for Mount St. Helens (M_{max}=1.5) and about 20 m for Crater Peak (M_{max}=0.6). These values are determined using standard scaling relations, such as those given by *Kanamori and Anderson* [1975]. The variations of the FMD are not affected by changes in the magnitude of completeness or the introduction of an upper magnitude cap. To address the question of whether the described anomalies could be caused by artifacts in the magnitude reporting or the hypocenter accuracy we investigated the dependency of a number of quality descriptors (such as RMS, vertical and horizontal error, number of stations reporting) on depth and magnitude. To create a high b-value anomaly one would have to deplete a volume of large earthquakes, thus enriching neighboring volumes with larger events. At Mount St. Helens we found no indication in the FMD that such a depletion/enrichment took place. The analysis at Mt. Spurr is less reliable due to the smaller number of earthquakes in the catalog, and the fact that the three eruptions in 1992 forced changes in the seismic network configuration. In addition, we find some indication that the larger events may be more susceptible to systematic mislocations, and the FMD's also indicate the presence of an enrichment/depletion (Fig. 3). A more systematic study of the location accuracy at a number of Alaskan volcanoes and the potential impact of systematic errors in the hypocenters and magnitudes is currently being performed (*A. Jolly*, pers. comm., 1996).

We believe that the spatial mapping techniques applied in this paper can give important clues about the plumbing system of a volcano. The FMD is one of the few methods available for collecting information about the material properties at depth, short of drilling. Future work will focus on more case studies, a better understanding of the influence of random and systematic errors in hypocenter location, and an attempt to analyze the FMD as a function of time and space simultaneously. To overcome the ambiguity in the interpretation of *b*-value changes, it is necessary to quantitatively compare these changes with other geophysical and petrological observations such as attenuation, P- and S-wave velocities, stress tensor orientations, and earthquake swarm locations at a variety of volcanoes.

Acknowledgments: The authors would like to thank A. Jolly, M. Wyss, C. Nye, H. Fletcher, J. Benoit, and two anonymous reviewers for comments. Additional thanks to the University of Washington for providing the earthquake catalog. This work has been partially supported through a dissertation fellowship of the University of Alaska Fairbanks (SW). A portion of this work was supported by the U.S. Geological Survey as part of the volcano Hazards and Geothermal Studies Program, and by additional funds from the State of Alaska through the Alaska Volcano Observatory (SM).

References

Alaska Volcano Observatory, Mt. Spurr 1992 Eruption, *EOS, Transactions AGU, 74,* 19. 217-222, 1993.

Barker, S., and S. Malone, Magmatic system geometry at Mount St. Helens modeled from the stress field associated with posteruptive earthquakes, *J. Geophys. Res., 96,* 11,883-11,894, 1991.

Bender, B., Maximum likelihood estimation of b-values for magnitude grouped data, *Bull. Seism. Soc. Am., 73,* 831-851, 1983.

Chadwick, W.W. Jr. , R.J. Archuleta, and D.A. Swanson, The mechanics of ground deformation precursory to dome-building extrusions at Mount St. Helens, 1981-1982, *J. Geophys. Res., 93,* 4351-4366, 1988.

Eichelberger, J.C., Silicic volcanism: Ascent of viscous magmas from crustal reservoirs, *Annu. Rev. Earth Planet. Sci., 23,* 41-63, 1995.

Gutenberg, B., and C.F. Richter, Frequency of earthquakes in California, *Bull. Seism.. Soc. Am., 34,* 185-188, 1944.

Ishimoto, M., and K. Iida, Observations sur les seisms enregistre par le microseismograph construit dernierment, *Bull. Earthq. Res. Inst. Tokyo Univ., 17,* 443-478, 1939.

Iyer, H.M., Geophysical evidence for the locations, shapes and sizes, and internal structures of magma chambers beneath regions of Quaternary volcanism, *Phil. Trans. R. Soc. Lond., A 310,* 473-510, 1984.

Kanamori, H., and D.L. Anderson, Theoretical basis of some empirical relations in seismology, *Bull. Seism. Soc. Am., 65,* 1073-1095, 1975.

Lees, J.M., The magma system at Mt. St., Helens: non-linear high-resolution P-wave tomography, *J. Volcanol. Geotherm. Res., 53,* 103-116, 1992.

Main, I.G., A characteristic earthquake model of the seismicity preceding the eruption of Mount St. Helens on 18 May 1980, *Phys. Earth Planet. Int., 49,* 283-293, 1987.

Mogi, K., Magnitude-Frequency relation for elastic shocks accompanying fractures of various materials and some related problems in earthquakes, *Bull. Earthq. Res. Inst., 40,* 831-853, 1962.

Moran, S., Seismicity at Mount St. Helens, 1987-1992: Evidence for repressurizing of an active magmatic system, *J. Geophys. Res., 99,* 4341-4354, 1994.

Nye, C.J., M.L. Harbin, T.P. Miller, S.E. Swanson, and C.A. Neal, Whole-rock major- and trace-element chemistry of 1992 ejecta from Crater Peak, Mount Spurr Volcano, Alaska, *USGS Bull. 2139,* 119-128, 1995.

Pallister, J., R. Hoblitt, D. Crandell, and D. Mullineaux, Mount St. Helens a decade after the 1980 eruptions: magmatic models, chemical cycles and a revised hazard assessment, *Bull. of Volcanol., 54,* 126-146, 1992.

Power, J.A, A.D. Jolly, R.A. Page, and S.R. McNutt, Seismicity and forecasting of the 1992 eruptions of Crater Peak vent, Mount Spurr volcano, Alaska: An overview, *USGS Bull. 2139,* 149-159, 1995.

Scandone, R., and S.D. Malone, Magma supply, magma discharge and readjustment of the feeding system at Mount St. Helens during 1980, *J. Volcanol. Geotherm, Res., 23,* 239-362, 1985.

Urbancic, T.I., C.I. Trifu, J.M. Long, and R.P. Young, Space-time correlations of b values with stress release, *PAGEOPH. 139,* 449-462, 1992.

Utsu, T., On seismicity, in: Report of Cooperative Research of the Institute of Statistical Mathematics 34, Mathematical Seismology VII, *Annals of the Institute of Statistical Mathematics, Tokyo,* 139-157, 1992.

Warren, N.W., and G.V. Latham. An Experimental Study of Thermally Induced Microfracturing and its Relation to Volcanic Seismicity. *J. Geophys Res., 75,* 4455-4464, 1970.

Wiemer, S., and J. Benoit, Mapping the b-value Anomaly at 100 km Depth in the Alaska and New Zealand Subduction Zones, *Geophys. Res. Letters, 23,* 1557-1560, 1996.

Zobin, V.M., Variations of volcanic earthquake source parameters before volcanic eruptions, *J. Volcanol. Geotherm. Res., 6,* 279-293, 1979.

Stefan Wiemer and Stephen R. McNutt, Geophysical Institute, University of Alaska Fairbanks AK 99775-7320 e-mail: stefan@giseis.alaska.edu, steve@giseis.alaska.edu

(Received June 24, 1996; revised November 15, 1996; accepted November 18,1996.)